HUNGARIAN AGRICULTURAL ENGINEERING
N° 34/2018 5-10
Published online: http://hae-journals.org/
HU ISSN 0864-7410 (Print) / HU ISSN 2415-9751(Online)
DOI: 10.17676/HAE.2018.34.5
Research Article
Received: 2018.06.02.; Accepted: 2018.10.18.

PERIODICAL OF THE COMITTEE OF AGRICULTURAL AND BIOSYSTEM ENGINEERING OF
THE HUNGARIAN ACADEMY OF SCIENCES
and
SZENT ISTVÁN UNIVERSITY
Faculty of Mechanical Engineering

ANALYSATION OF THE EFFECT OF THE CONTACT PARAMETERS ON SOIL'S SHEAR BEHAVIOUR IN DISCRETE ELEMENT SIMULATIONS

Author(s):
K. Kotrocz – Gy. Kerényi

Affiliation:
Budapest University of Technology and Economics, Department of Machine and Product Design

Email address:
kotrocz.krisztian@gt3.bme.hu, kerenyi.gyorgy@gt3.bme.hu

Abstract

Direct shear tests are commonly used in agricultural research to determine the soil's cohesion and internal friction angle. This phenomenon can be modelled using the Discrete Element Method (DEM) very well. In this paper the results of numerical discrete element simulations were presented. The aim of the calculations was to analyse the effect of the Hertz-Mindlin with bonding contact properties on shear force-shear displacement curve. Using these results the contact parameters can be set up to reach similar results in the discrete element simulations and real direct shear test.

Keywords

DEM, direct shear test, Hertz-Mindlin with bonding contact model

1. Introduction

Soil shear behaviour plays an important role in agricultural researches because soils are under significant shear stress when traction force is generated by the driven wheels of the tractors or trucks [1, 2, 3]. Therefore, the mechanical properties of the soil, namely the cohesion and the internal friction angle are important parameters which can be used in the design process of these machines to reduce the stress applied into the soil during tillage operations. One of the most common methods to measure these properties is the laboratory direct shear box test [1, 2, 3].

Discrete Element Method (DEM) was developed in the last century by Cundall and Strack [4] and is widely used in the literature to model cohesive and non-cohesive materials such as soil [5, 6, 7]. In most researches the Hertz-Mindlin contact models are used to simulate soil cutting [5], wheel-rolling [7] etc. where numerical direct shear tests are presented to calibrate the soil material. However, Safranyik investigated the effect of the Hertz-Mindlin with bonding contact properties on soil's cohesion and internal friction angle [8], but there is no publication about the effect of these contact properties on the shear force-shear displacement curve yet. Therefore, the aim of this work to investigate these phenomena.

2. Materials and Methods

In DEM, the importance of the contact models is very high because in most cases only rigid particles are used in the simulations. In this paper the Hertz-Mindlin with bonding contact model was used to model cohesive soil which consists two separate model. The Hertz-Mindlin model [9, 10, 11] is present to model the friction and pressure between the particles and the Parallel Bond model [12] is responsible to simulate the cohesion in the soil.

By using the Hertz-Mindlin contact model the contact force can be divided into normal and shear forces according to the normal and tangential direction of the contact. The contact normal force (F_n) between the particles can be calculated from the normal overlap of the elements (δ_n) by Eq. 1:

$$F_n = \frac{4}{3} \cdot E^* \cdot \sqrt{R^*} \cdot \delta_n^{\frac{3}{2}}. \quad (1)$$

The E* denote to equivalent elastic modulus and R* is the equivalent radius. These can be determined from the parameters, E and R of the contacting particles. In addition, the contact shear force (F_t) can be calculated as:

$$F_t = -S_t \cdot \delta_t = -8 \cdot G^* \cdot \sqrt{R^* \cdot \delta_n} \cdot \delta_t, \quad (2)$$

where G* is the equivalent shear modulus and δ_t is the tangential overlap of the elements. The shear force has a limit; it cannot be greater than the value from Eq. 3 which represents the Coulomb-friction criteria.

$$F_t \leq F_n \cdot \mu_s. \quad (3)$$

In addition, there are damping forces, in normal (F_{nd}) and tangential direction (F_{td}) as well to model the energy dissipation of the collision:

$$F_n^d = -2 \cdot \sqrt{\frac{5}{6}} \cdot \beta \cdot \sqrt{S_n \cdot m^*} \cdot v_n^{rel}, \quad (4)$$

$$F_t^d = -2 \cdot \sqrt{\frac{5}{6}} \cdot \beta \cdot \sqrt{S_t \cdot m^*} \cdot v_t^{rel}, \quad (5)$$

where β can be calculated by Eq. 6 using the coefficient of restitution (e).

$$\beta = \frac{\ln e}{\sqrt{\ln^2 e + \pi^2}} \tag{6}$$

Once the Parallel Bond is formed between the particles, a set of elastic springs are created around the contact point with Bond radius of R^B. The Bond model acts parallel with the Hertz-Mindlin contact model, therefore additional normal (ΔF_n) and shear (ΔF_t) forces are summed to the corresponding components:

$$\Delta F_n = -S_n^B \cdot A \cdot \Delta\delta_n, \tag{7}$$

$$\Delta F_t = -S_t^B \cdot A \cdot \Delta\delta_t, \tag{8}$$

These can be calculated from the cross section (A), the normal (S_n^B) and tangential stiffness (S_t^B) of the Bond and the relative normal ($\Delta\delta_n$) and tangential displacements ($\Delta\delta_t$) of the contacting particles. With Parallel Bonds, moments can be transmitted through the elements in normal and shear direction as well. The value of these moments can be determined from the polar moments of inertia of the Bond (J) and from the particles relative normal ($\Delta\theta_n$) and tangential rotations ($\Delta\theta_t$).

$$\Delta M_n = -S_n^B \cdot J \cdot \Delta\theta_n, \tag{9}$$

$$\Delta M_t = -S_t^B \cdot \frac{J}{2} \cdot \Delta\theta_t, \tag{10}$$

Note that the relative displacements and rotations are set to zero when the Bond is defined at the time of tBond. Each Bond has a limit value of stress (i.e. the Bond's normal (σmax) and shear strength (τmax)) and if one of these limits are obtained, the Bond will break and from the next timestep the contacting particles will move according to the Hertz-Mindlin contact model only. The maximum of the stresses in the Bond can be calculated by Eq. 11 and Eq. 12.

$$\sigma_{max} = \frac{-\Delta F_n}{A} + \frac{2 \cdot M_t}{J} \cdot R^B \tag{11}$$

$$\tau_{max} = \frac{-\Delta F_t}{A} + \frac{M_n}{J} \cdot R^B \tag{12}$$

In DEM, the simulating process is divided into small timesteps of dt, and in each timestep the elements' displacement-vectors (including the translations and rotations of the particles) are calculated according to Newton 2nd law. The value of dt has great effect on simulation results, it should be small enough to capture great impacts between the elements. But by choosing small timestep, the calculation time will be increased dramatically. To set up the correct value of the timestep, the EDEM User Manual [13] makes a suggestion, namely it should be in the range of 0.1… 0.2 times of the Rayleigh timestep ($t_{Rayleigh}$). In our simulations this was taken into account which resulted that the calculations were performed with timestep of 5e-06 s.

3. Real direct shear test and discrete element simulations

To compare the results of the discrete element simulation with real measurement values, direct shear tests were conducted in the laboratory of the Szent István University of Gödöllő, Institute of Process Engineering. First the soil samples were transported to the laboratory in core cylinders, and after that the tests were carried out using the ELE 26-2112/01 type direct shear apparatus (Figure 1). The samples were loaded vertically with the load force of 400 N, and the shearing process was started with the speed of 5 mm/min. During the process, the force acting on the top cylinder of the shear box assembly (as shear force) and the horizontal displacement of the top cylinder (as shear displacement) were measured. Note that the vertical displacement of the samples was not measured during the measurements. The diameter and the height of the top and bottom cylinder as well were 60 mm and 12,7 mm, respectively.

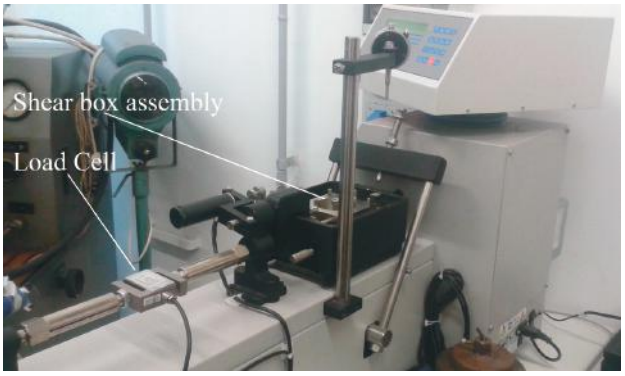

Figure 1. The ELE 26-2112/01 type direct shear apparatus.

The same geometry of shear box assembly where created in EDEM 2.7 software environment. The cylinders were filled with spherical elements with radius of 1,33…3 mm, and after the whole system obtained the equilibrium state (the maximum of the elements velocity got smaller than 0,01 mm/s) the Parallel Bonds were installed between the particles. Then the vertical force of 400 N (i.e. the normal load) was applied on to the top of the model through a clump element, shown as grey colour in Figure 2. Finally, the top section of the assembly was moved horizontally with the speed of 50 mm/s which is 10 times higher than the used shearing speed in real direct shear tests. This was chosen to minimize the calculation time of the discrete element simulations and according to our earlier research it has negligible effect on the results.

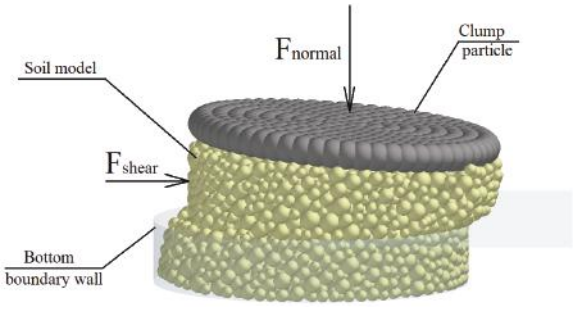

Figure 2. Numerical direct shear tests.

Some of the contact properties of the first model (shown in Table 1) were set up according to the calibration process presented in our earlier research [14] and the remaining contact parameters were chosen for sensitivity test:

- particle's shear modulus,
- particle's Poisson-ratio,
- particle's density,
- Parallel Bond radius, and
- Parallel Bond stiffness.

Table 1. The properties of the first discrete element soil model

Parameter	Value
Geometrical properties	
Particle radius distribution (mm)	1,33…3
Contact radius (mm)	1,6…3,6
Initial porosity (before the normal load applied) (-)	0,425
Properties of the Hertz-Mindlin with bonding contact model between the soil elements	
Density (kg/m^3)	1,8e+03
Shear modulus (Pa)	1,44e+07
Poisson ratio (-)	0,25
Coefficient of restitution between the soil particles (-)	0,5
Coefficient of restitution between the soil particles and walls (-)	0,5
Friction coefficient between ball and ball (-)	0,4
Friction coefficient between ball and walls (-)	0,6
Bond radius (mm)	1,5
Bond normal stiffness (Pa/m)	9,5e+06
Bond shear stiffness (Pa/m)	9,5e+06
Bond normal strength (Pa)	3,131e+4
Bond shear strength (Pa)	4,428e+4
Properties of the Hertz-Mindlin contact model between the cylinder (wall) elements	
Density (kg/m^3)	7,8e+03
Shear modulus (Pa)	7,692e+10
Poisson ratio (-)	0,3
Coefficient of restitution between walls (-)	0,5
Friction coefficient between wall and wall (-)	0,1

Discrete element simulations were performed with different values of these properties (Table 2) and their effect on simulation results, namely the shear force-shear displacement curve were analysed. Our aim was to determine which contact parameters have significant effect on the process of soil shearing and therefore is necessary to take into account while calibrating the properties of the soil model to the measurement results.

Table 2. The value of the contact properties in the sensitivity test.

Parameter	Range of value
Shear modulus (Pa)	1,44e+06… 1,4e+08
Poisson ratio (-)	0,2…0,3
Density (kg/m^3)	1,6e+03… 2,0e+03
Bond radius (mm)	0,5…3,0
Bond normal and shear stiffness (Pa/m)	9,5e+06… 4,75e+07

4. Results and Discussion

In this section, the results of the discrete element simulation are presented.

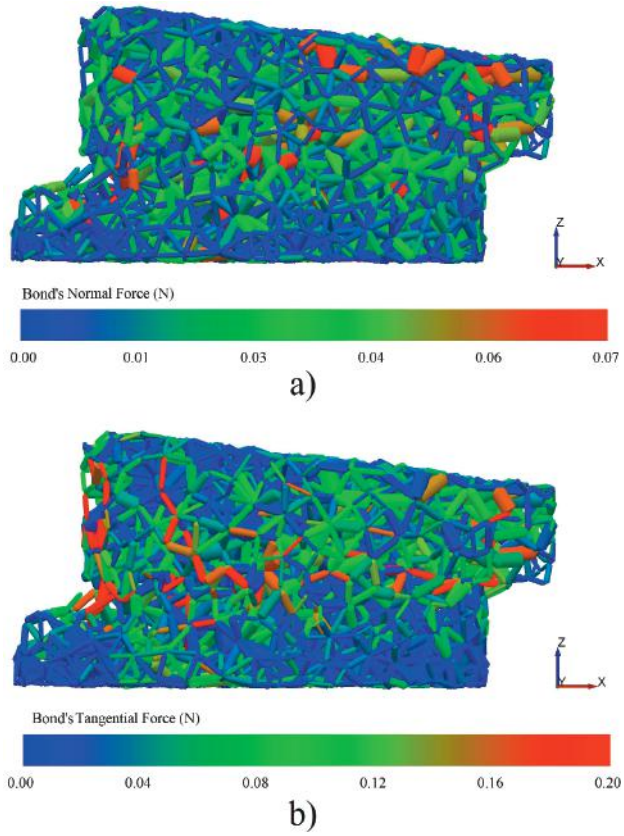

Figure 3. The Parallel Bonds between the particles.

First the results were checked qualitatively to be sure that the simulation process is similar to the real direct shear test. Thus, the Parallel Bonds with their normal and tangential forces and moments were investigated. In Figure 3, the Bonds between the elements are shown as beams, and are coloured according to the Bond's normal and tangential force in the part of the figure a) and b), respectively. It can be seen that the highest forces arise in the shear zone and on the top of the soil, where the normal load is applied. We concluded that the axial and shear moments in the bonds are much smaller, thus has negligible effect on the normal and shear stresses on the Bond according to Eq. 11 and Eq. 12.

So it can be asserted that the highest Bond's stresses arise near the shear zone which is a good result when comparing the calculations to the theoretical process.

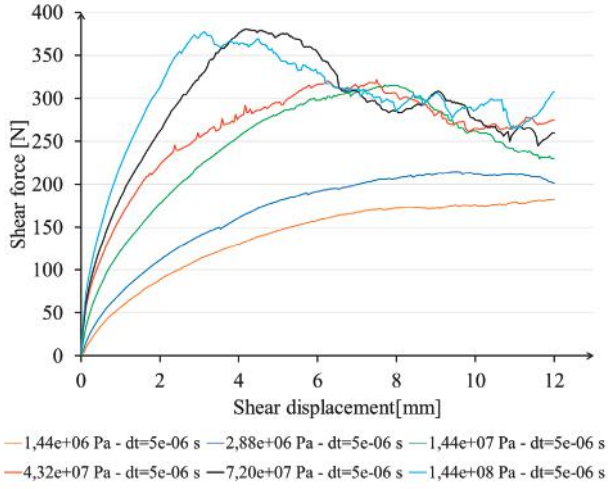

Figure 4. Effect of the particle's shear modulus.

In Figure 4, the effect of the particle's shear modulus is shown. It can be clearly seen that this property has great effect on the shear force-shear displacement curve. By increasing the value of the shear modulus, the maximum of the shear force is increasing as well while the displacement, where these maximum forces arise, is reducing. According to these results, it can be asserted that the shear modulus of the elements has great effect on the gradient of the curve. Note that in case of shear modulus value of 1,44e+07…4,32e+07 Pa the characteristic of the curve is changing; in case of smaller shear modulus one can get the so-called asymptotic shear force-shear displacement curve which is typical in case of loose or non-cohesive soils [1, 2, 3]. On the other hand, in case of high particle's shear modulus, the curve has high peak forces which can be measured in cemented, cohesive soils [1, 2, 3].

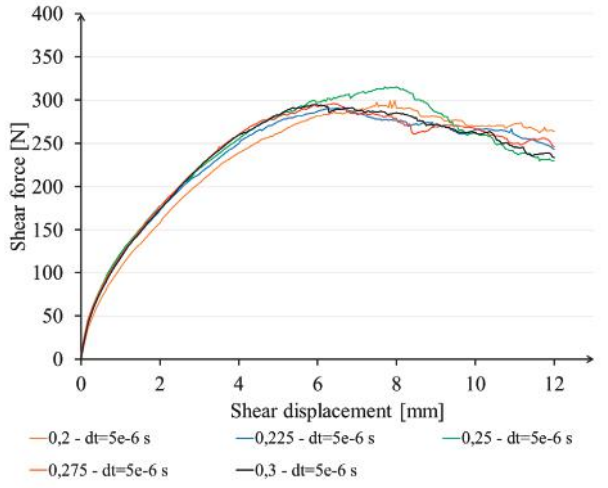

Figure 5. Effect of the particle's Poisson ratio.

After the shear modulus, the Poisson ratio and the density of the particles were analysed, the results can be seen in Figure 5 and Figure 6. It can be asserted that in the range of value of these contact properties, there is no significant effect on the shear force-shear displacement curve.

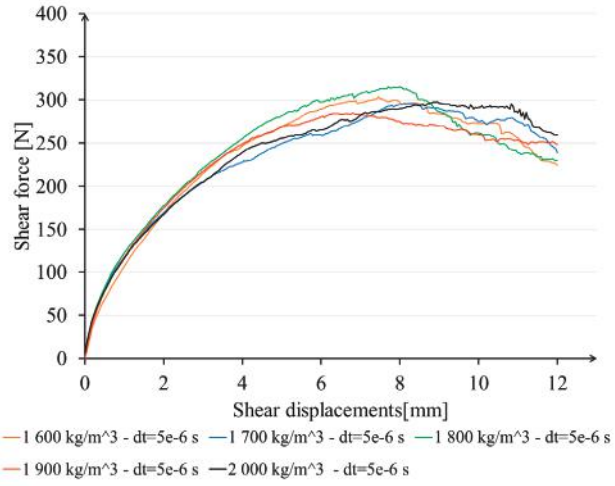

Figure 6. Effect of the particle's density.

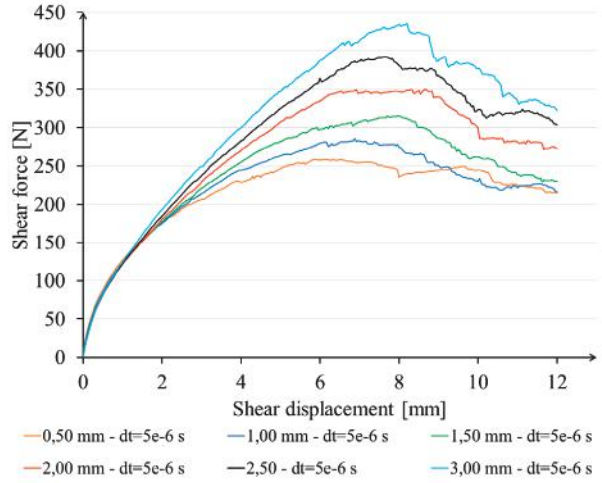

Figure 7. Effect of the Bond radius.

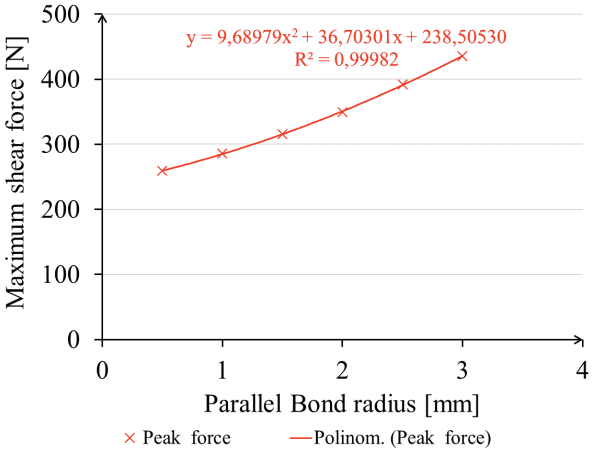

Figure 8. Effect of the Bond radius on the maximum of the shear forces.

Finally, the properties of the Parallel Bond contact model, namely the Bond radius and stiffness were analysed. In Figure 7, it can be seen that by increasing the Bond radius, the peak force

and the displacement, where these forces occur, is increasing as well. But this contact parameter has negligible effect on the gradient of the curve in the range of shear displacement of 0…2 mm. In Figure 8, the peak forces are presented in a function of Parallel Bond radius. It is shown that a quadratic polynomial curve can be fitted to the points with high value of R2 using the Ordinary Least Squares method. This can be used further to estimate the value of the peak force in case of varying Parallel Bond radius. Note that the quadratic polynomial curve was chosen because according to Eq. 7 and Eq. 8, the normal and shear forces in the Bond is proportional to the area of the Bond, thus to the 2nd power of the Bond's radius.

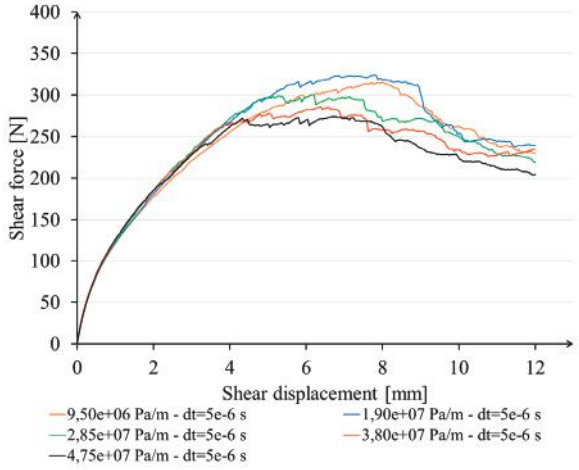

Figure 9. Effect of the Bond stiffness.

In Figure 9, the effect of the Bond's stiffness is shown. By changing the value of this parameter, the shear force-shear displacement curve is modified a little bit, the peak force is slightly different in the investigated five cases. But this difference is negligible, the first sections of the curves (in the range of displacement of zero to 4 mm) are almost exactly the same. So we concluded that this parameter is not so important in the calibration process of cohesive soils as the particle's shear modulus and the radius of the Parallel Bond were.

After the effect of the contact parameters was determined, our aim was to calibrate the properties of the model to the shear force-shear displacement curve, measured during the laboratory direct shear tests. So the Parallel Bond radius and the shear modulus of the particles were set up correctly (Table 3), the other parameters remained the same as were in the first model.

Table 3. The calibrated value of the contact properties derived from the results of the sensitivity test.

Parameter	Range of value
Shear modulus (Pa)	1,488e+07
Poisson ratio (-)	0,25
Bulk density (kg/m^3)	1,8e+03
Bond radius (mm)	0,93
Bond normal and shear stiffness (Pa/m)	9,5e+06

Figure 10 shows the results of the simulation observed with the calibrated/final contact properties. Up to the displacement of 10 mm the shear force-shear displacement curves from the calculation and measurement are very similar which is a very good result. This means that this soil model is able to simulate the failure of cohesive soil properly, thus can be used in all cases, where the normal load of the soil is similar to the load in the direct shear test (e. g. in case of wheel rolling on deformable soil with similar vertical load).

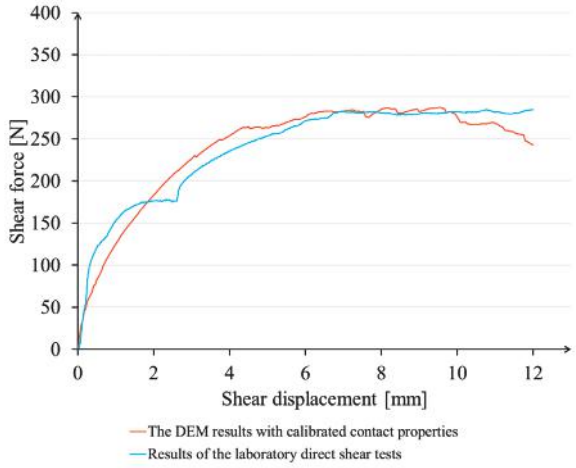

Figure 10. Comparison of the shear force-displacement curves from the measurement and from the simulations.

5. Conclusion

In this paper the discrete element method was adapted to simulate cohesive soil's direct shear test. The aim of our work was to determine those properties of the Hertz-Mindlin with bonding contact model, which has significant effect on shear force-shear displacement curve. As a results, we concluded that these parameters were the particle's shear modulus and Parallel Bond radius. The other investigated parameters (including the Poisson-ratio, the density of the elements and the Parallel Bond stiffness) has negligible effect on soil shearing process, thus can be ignored while calibrating the discrete element model to the result of real measurements. The remaining contact properties can be set up using our earlier research.

The soil model with final contact properties was able the simulate the real direct shear test properly, thus it can be used in additional simulations where soil shearing plays important role (i. e. wheel rolling, soil cutting). On the other hand, the results can be used to develop a calibration process for direct shear simulations.

Acknowledgements

The authors will gratefully acknowledge the assistance of the staff of Institute of Process Engineering, Szent István University of Gödöllő to provide their direct shear apparatus for the measurements.

The research reported in this paper was supported by the Higher Education Excellence Program of the Ministry of Human Capacities in the frame of Artificial intelligence research area of Budapest University of Technology and Economics (BME FIKP-MI).

References

[1] Laib, L. (Ed.): 2002. Terepen mozgó járművek (Moving off-road vehicles). Szaktudás Kiadó Ház, Budapest (in Hungarian).
[2] McKyes, E.: 1985. Soil Cutting and Tillage. The University of Michigan, Michigan.
[3] Sitkei, Gy.: 1967. A mezőgazdasági gépek talajmechanikai problémái (The soil's mechanical problems of the agricultural machines). Akadémia Kiadó, Budapest (in Hungarian).

[4] Cundall, P. A., Strack, O.D.L.: 1979. A discrete numerical model for granular assemblies. Géotechnique, Vol. 29. pp. 47-65.
[5] Chen, Y., Munkholm, L. J., Nyord, T.: 2013. A discrete element model for soil–sweep interaction in three different soils. Soil & Tillage Research, Vol. 126. pp. 34-41. http://dx.doi.org/10.1016/j.still.2012.08.008
[6] Keppler, I., Kocsis, L., Oldal, I., Csatár, A.: 2011. Determination of the discrete element model parameters of granular materials. Hungarian Agricultural Engineering, Vol. 23. pp. 30-32.
[7] Smith, W., Melanz, D., Senatore, C., Iagnemma, K., Peng, H.: 2014. Comparison of discrete element method and traditional modeling methods for steady-state wheel-terrain interaction of small vehicles. Journal of Terramechanics, Vol. 56. pp. 61-75. http://dx.doi.org/10.1016/j.jterra.2014.08.004
[8] Safranyik, F.: 2016. Silók gravitációs és vibrációs ürítése (Gravitational and vibrational discharge of silos). Ph.D. thesis. Gödöllő (in Hungarian).
[9] Hertz, H.: 1882. On the contact of elastic solids. J. reine und angewandte Mathematik, Vol. 92. pp. 156-171.
[10] Mindlin, R. D.: 1949. Compliance of elastic bodies in contact. Journal of Applied Mechanics, Vol. 16. pp. 259-268.
[11] Mindlin, R. D., Deresiewicz, H.: 1953. Elastic spheres in contact under varying oblique forces. ASME pp. 327-344.
[12] Potyondy, D. O., Cundall, P. A.: 2004. A bonded-particle model for rock. International Journal of Rock Mechanics and Mining Sciences, Rock Mechanics Results from the Underground Research Laboratory, Canada, Vol. 41. pp. 1329-1364. http://dx.doi.org/10.1016/j.ijrmms.2004.09.011
[13] EDEM 2.7 User Guide: 2015. DEM Solutions Ltd.
[14] Kotrocz, K., Kerényi, Gy.: 2017. Numerical Discrete Element Simulation Of Soil Direct Shear Test, 31st Conference on Modelling and Simulation, ECMS 2017, Budapest, Hungary, pp. 510-515. Edited by: Zita Zoltay Paprika, Péter Horák, Kata Váradi, Péter Tamás Zwierczyk, Ágnes Vidovics-Dancs, János Péter Rádics. http://dx.doi.org/10.7148/2017-0510